

# Bearing capacity spectra for steel structures

Aleksandar Juriač<sup>(1)</sup> and Ante Mihanović<sup>(2)</sup>

<sup>(1)</sup>Faculty of Civil Engineering, University Josip Juraj Strossmayer of Osijek, Drinska 16a, HR-31000 Osijek, CROATIA, e-mail: ajuric@gfos.hr

<sup>(2)</sup>Faculty of Civil Engineering, University of Split, Matice hrvatske 15, HR-21000 Split, CROATIA e-mail: Ante.Mihanovic@gradst.hr

## SUMMARY

*This paper presents a method for obtaining bearing capacity spectra through the analysis of the stability of column steel structure elements by means of a material and geometrically nonlinear model. Diagram spectra are shown non-dimensionally for each group of sections, and they present the dependence of slenderness and failure load on the given eccentricity. The analysis results are compared to prevalent steel structure stability standards and they show minimal deviations. No special engineer training or knowledge is demanded for diagrams what makes them applicable in engineering practice. In relation to standard computations, the usage of diagrams obtained by considering material and geometrical nonlinearity enables more rational material and structure exploitation.*

**Key words:** material and geometrical nonlinearity, bearing capacity spectra, steel structures, stability analysis.

## 1. INTRODUCTION

The computation of the stability and bearing capacity of truss and frame steel structures whose elements are most often exposed to centric and eccentric compressive loads, almost always implies the influence of material and geometrical nonlinearity. Although there are rigorous numerical models for the analysis of such structures today [1-5], their everyday usage is mostly nonrational due to the high cost of training experts to master those models and to the relatively low price of standard steel linear structures.

Therefore the authors suggest the usage of nondimensional spectra of bearing capacity diagrams for determining the bearing capacity of linear element structures exposed to both centric and eccentric pressure from the stability aspect. Diagram spectra of the bearing capacity and stability cover the field of both the centric and eccentric pressure with lower and higher eccentricity as well as the field of slenderness according to the standard technical regulations. They are developed by numerical tests performed of simple examples of columns with different forms of the profiles. They result from the highly precise numerical analysis of the stability and bearing capacity of the characteristic column and are based on the numerical model of the material and geometrical nonlinearity

according to the theory of small displacements. The diagrams are defined by non-dimensional rates and are widely applicable in the engineering practice.

## 2. NONLINEAR NUMERICAL MODEL

The model can be successfully applied for solving problems in the field of plane truss and frame structures. Since the stability problem cannot be solved by analytical computation, some other methods are applied in the model which give sufficiently precise or approximate solutions. The solution implies the determination of the failure load which leads to the loss of stability and failure of the structure.

In nonlinear equations the stiffness matrix consists of the stiffness matrix obtained by the linear theory of small displacements  $\mathbf{K}_o$ , the so-called basic stiffness matrix and the stiffness matrix according to the nonlinear theory of small displacements  $\mathbf{K}_g$ , the so-called geometrical stiffness matrix.

The equation of a nonlinear system can be presented in the following way:

$$(\mathbf{K}_o + \mathbf{K}_g(u)) \cdot \mathbf{u} = \mathbf{F}(u) \quad (1)$$

Hereby we obtain a system of nonlinear equations soluble by approximate numerical methods, which

formulated by the finite element method, provides good solution convergence.

The analyzed column-beam structure is discretized by 1D finite elements (Figure 1). Each finite element is joined to its local co-ordinate system, whereas the whole structure can be examined in the global co-ordinate system.

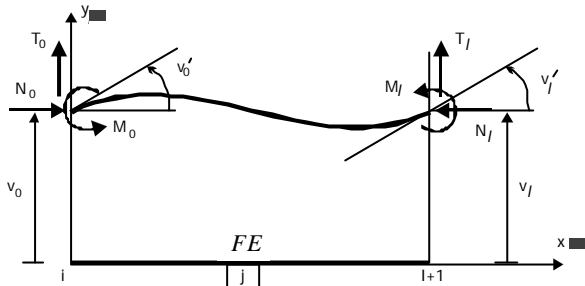


Fig. 1 Forces and displacements of a finite element (FE)

The approximate solution on one-dimensional linear finite element is constructed by shape base  $H$  functions chosen as Hermit's polynomials of the first and third order. By combining these functions we get combined or global base functions which can be used to present shear and flexural displacements.

### 2.1 Modelling of the geometrical nonlinearity

The influence of the geometrical nonlinearity is simulated by achieving a balance of a strained structure on the deformed position (Figure 2). The equations we use differ from those used in the initial geometry and they are nonlinear.

Total Lagrange's formulation is used.

Geometrical nonlinearity exerts its influence on the assumption that:

- a theory of small displacements is applied;
- the members are prismatic in parts with a constant section and ideally straight;
- elements are deformed axially, flexurally and by shear;
- equilibrium is established on the deformed system;
- gravity type of loading.

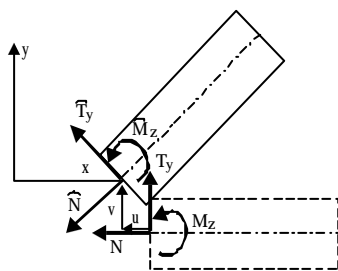


Fig. 2 Displacements of elements' cross-sections

If we choose displacements from the group of  $H$  functions, which give a close solution, then from the equation of external and internal forces it follows:

$$s^e = [k_o^e + k_g^e(u)] u - F^e(u) \quad (2)$$

where  $k_o^e$  is the basic stiffness matrix,  $k_g^e$  is the geometrical stiffness rigidity and  $F^e$  is the vector of the wedging force.

By transforming the local co-ordinate system into the global one we set conditions of compatibility of node displacements. This condition keeps node forces in balance which is also the balance of the global system:

$$[K_o + K_g(u)] u = F(u) \quad (3)$$

where the global matrices of basic and geometrical stiffness and load vector are:

$$K_o = \sum k_{o_{GL}}^e, \quad K_g(u) = \sum k_{g_{GL}}^e, \quad F(u) = \sum F_{GL}^e \quad (4)$$

### 2.2 Modelling of the material nonlinearity

Material nonlinearity exerts its influence on the assumption that:

- a theory of small deformations is applied;
- nonlinear relation between stresses and strains;
- a layered cross-section model is used.

Compared to the linear elastic theory nonlinearity significantly affects the behaviour of engineering structures. This model is based on the efficient simulation of the constant nonlinearity as well as on the height of the section.

A layered cross-section model is used for the simulation (Figure 3).

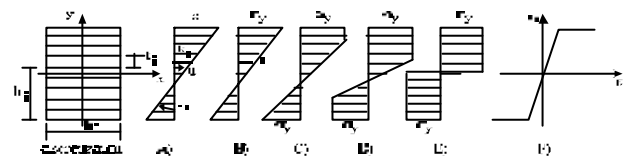


Fig. 3 A model of cross-section yielding

The cross-section is discretized by thin layers defined by the thickness, width and sort of a material (if there are two or more). The behaviour of the whole layer is determined by the behaviour of the middle point of the layer in which uni-axial strain is examined.

The material is described by the  $s$ - $e$  diagram which is given by the finite number of discrete points. The steel model Fe 360 is illustrated in Figure 4.

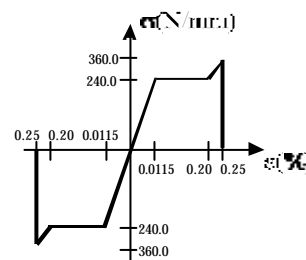


Fig. 4 Idealized  $s$ - $e$  diagram for steel Fe 360

The Navier hypothesis is valid so that deformations can be described by  $u$  and  $f$  parameters.

Figures 3 b) to e) illustrate the development of the cross-section yielding due to the bending moment and compressive axial force.

Figure 3 f) represents the idealized elasto-plastic  $s$ - $e$  diagram.

Section yielding  $F(N,M)=I$  is conditioned by the natural diagram of the cross-section bearing capacity which can be determined by the numerical method for the appertaining cross-section per layered model.

The balancing of the cross-section for the given cross-section combinations  $N$  and  $M$  is carried out iteratively and it is used for testing the stage of the cross-section deformation (linear, nonlinear, yielding stage, or failure) [6].

With nonlinear examples we use the direct iterative method for solving the nonlinear problems.

A thick net of FE is required for the adequate stimulation of constant material nonlinearity and yielding along the structure elements. One possibility is to divide finite elements into the equal number  $R$  of sub-elements (sub-element = SE).

For each SE, flexural and axial stiffnesses (EI, EA) are accepted as constants for the given load increment and iterative step of balancing the structure. The stiffness is determined in the referential cross-section, i.e., in the intergration point whose position is measured from the beginning of FE for the considered sub-element, given by the expression:

$$x = \frac{l(r-1)}{R-1} \quad (5)$$

where  $l$  is the length of the finite element,  $r$  is the number of the given sub-element, and  $R$  is the total number of SE on FE. In this way the initial and finite cross-sections FE are always included [6].

This numerical method is very accuracy sensitive, so it is recommendable to adopt  $10 < R < 30$ .

It is necessary for the discretization method to assure sufficient accuracy since each structure discretization on FE leads to certain errors of the numerical method.

### 2.3 Incremental iterative algorithm

The loss of the stability, i.e., bearing capacity of the structure is expressed by the critical parameter  $f_k$ . To determine the critical parameter  $f_k$  we apply incremental iterative methods whose basic principle is incremental loading along the sections, i.e. increments. Sufficiently dense increments provide the solution which will most likely correspond to the physical state.

The algorithm is as follows:

- for  $m$  - increment step in loading ( $F_m = f_m P_0$  where  $P_0$  is starting load)
- $n$  - iterative step in balancing:

1. Determination of the global stiffness matrix according to the section forces obtained for the proceeding iterative of increment step:

$$K_m^n = \sum (K_m^n)^e$$

2. Determination of the global load vector, which can be changed during iteration as finite element stiffness changes:

$$F_m^n = \sum (F_m^n)^e$$

3. Computation of new displacements:

$$v_m^n = \sum (K_m^n)^{-1} F_m^n$$

4. Iterative procedure is continued, if the displacement norm has not been satisfied.

Characteristic displacements are tested. If instability occurs, some of the characteristic displacements change the sign and displacement norm suddenly increases.

The calculation period depends on many parameters but for a well selected model it can be estimated to 10 increments with 10 iterations in each increment.

### 2.4 Accuracy of the numerical procedure

Incremental iterative algorithm and the described numerical model generate errors which can be classified as:

1. geometrical nonlinearity error  $e_{GD}$ , caused by discretization density and by the selection of the shape function over the finite element,
2. material nonlinearity error  $e_{MD}$ ,
3. iterative procedure error  $e_{IT}$ ,
4. incremental procedure error  $e_{IN}$ .

Total error of the model is expressed as the least favourable combination of individual errors:

$$e_T \leq e_{GD} + e_{MD} + e_{IT} + e_{IN} \quad (6)$$

In examples of steel structures, total error is mainly generated by the error of the input parameters of the displacement accuracy  $e_{u2}$ , the error of the section forces  $e_{u1}$  and the load increment  $i$ :

$$e_T = e_{u2} + i(1 + e_{u1}) \quad (7)$$

where  $e_{u1}$  is generally selected between 0.02 and 0.10,  $e_{u2}$  less than 0.03, and  $i=0.02$ . Assuming that  $e_{u1}=0.05$ ,  $e_{u2}=0.02$ , the total error is:  $e_T=0.02+0.02 \cdot (1+0.05)=0.041$ .

Since failure load is found mainly in one - half of the unrealized increment, the average error is:

$$e_{Tsr} = e_{u2} + \frac{1}{2}i + e_{u1} \cdot i \quad (8)$$

In the specific example the average error is:  $e_{Tsr}=0.02+0.01+0.001=0.031$ .

### 3. BEARING CAPACITY SPECTRA

The bearing capacity spectra result from the stability analysis and bearing capacity of individual linear elements of truss and frame steel structures. The analysis is based on the series of numerical experiments on slender elements which are subject to centric and eccentric compressive loads taking into consideration material and geometrical nonlinearity.

The parameters which influence the degree of the critical force are nonlinearity of the material, imperfection of the system and eccentric load activity.

The eccentricity of structure elements can be caused by the deviation of the cross-section dimensions (rolling tolerance), by the deviation of the column axis from the straight line as well as by the deviation of the centric force.

By eccentric loading, eccentricity and material nonlinearity are related, so that the length of buckling and slenderness become changable, dependent on the loading level due to the change of the cross-section stiffness.

Finally, it can be concluded that in the nonlinear field there are no explicit expressions and it is therefore necessary to give an approximate degree of the structure reaction.

The examined column structure with the used sections and its numerical model are illustrated in Figure 5.

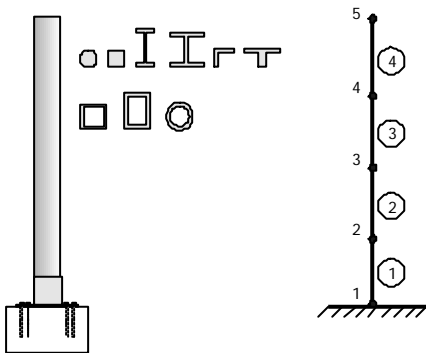


Fig. 5 Construction and discretized model of a steel column

The steel model is divided into four two-node straight FE with axial, flexural and shear stiffness. Each FE is divided into 20 SE. The computation is performed with the real Fe 360 characteristics.

In order to examine the load behaviour depending on the slenderness, the column height is varied equivalently to the slenderness  $I=0-300$  dependent on the cross-section form.

The column structure is exposed to the starting load  $N=10\text{ kN}$  which is varied together with the column length and the load system is illustrated in Figure 6.

In addition to this system there is also a combination of longitudinal and horizontal forces at the top of the column ( $e=Hh/N$ ) as well as a combination of longitudinal force and constant loading  $w$  along the column length ( $e=w\star h^2/2N$ ).

The chosen load system is less acceptable than these two because it can successfully substitute other systems of structure loading.

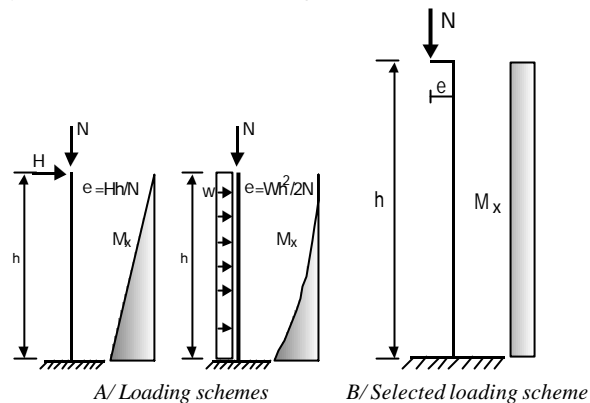


Fig. 6 System of an eccentric load column

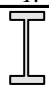

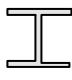

Several types of sections have been examined and the results are demonstrated as a non-dimensional diagram of the bearing capacity spectra for different eccentricity cases (Figures 7 to 10).

On the abscissa there is slenderness for linear-elastic materials and given load system and it is as follows  $I_0=l_{i0}/i_0$  where  $l_{i0}$  is the buckling length and  $i_0=\sqrt{I_0/A_0}$  is the initial inertia radius. On the ordinate there is a relation between the failure compressive load for the given eccentricity and the failure compressive load by choice of the short column  $v=N_k/N_0$ , and it is as follows  $e=e_0/i_0$ .

Consequently, the section form of steel structures affects the bearing capacity curves. Differences are particularly noticeable as eccentricity increases. Therefore, some sections can be grouped according to the same or a very similar form of bearing capacity curves as it is shown in Table 1.

Sections are grouped according to the curvature of bearing capacity curves for the eccentricities bigger than zero. As it can be seen from Table 1, the most curved bearing capacity curves have »high« I-sections, right after that all hollow sections, then I-sections and finally all full and unsymmetrical sections.

Table 1 Sections grouped according to the form of bearing capacity curves

Ordinal number	1.	2.	3.	4.
sections	 I-sections for $h > b$	 hollow sections	 I-sections for $h=b$	 solid and unsymmetrical sections

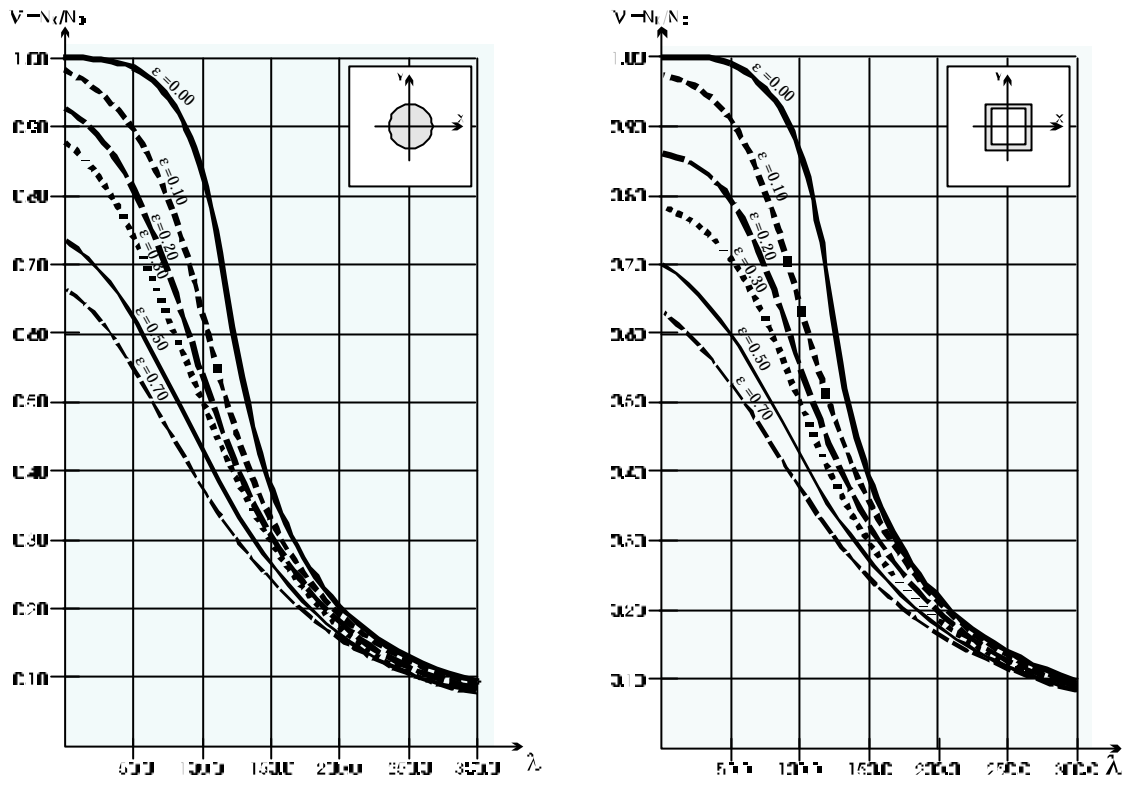


Fig. 7 Bearing capacity spectra of a steel column for the full circle and a hollow square section [7]

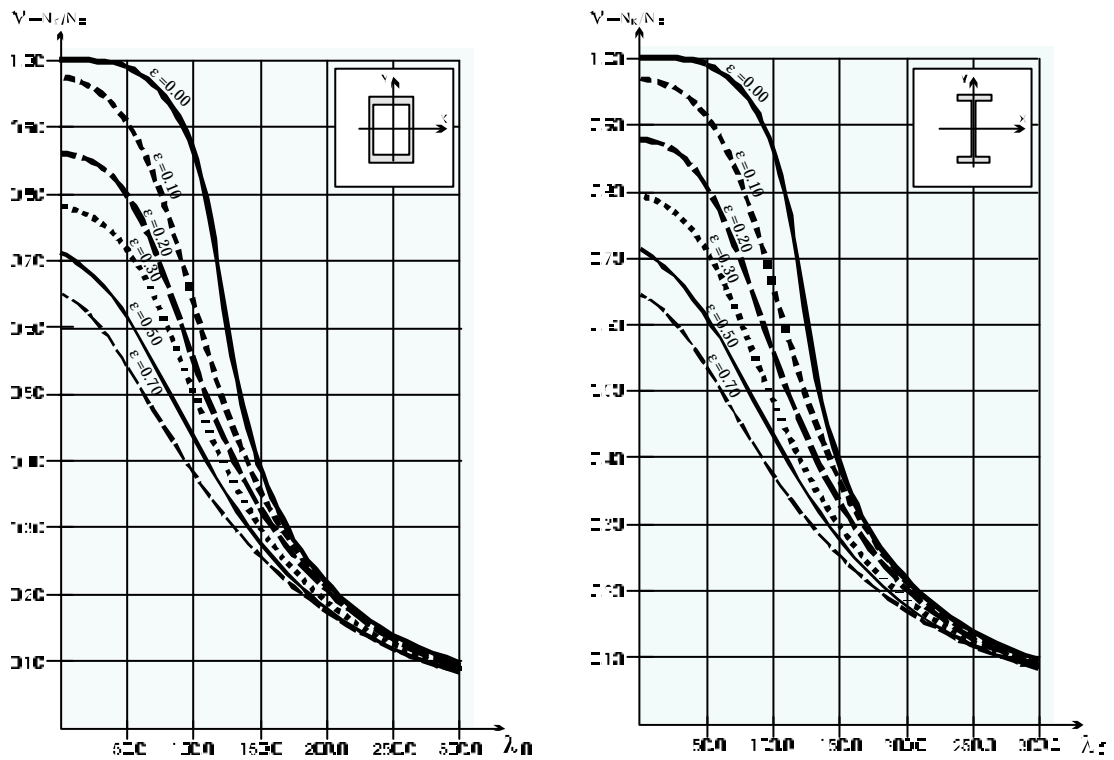


Fig. 8 Bearing capacity spectra for the hollow rectangular and I-section ( $h > b$ ) [7]

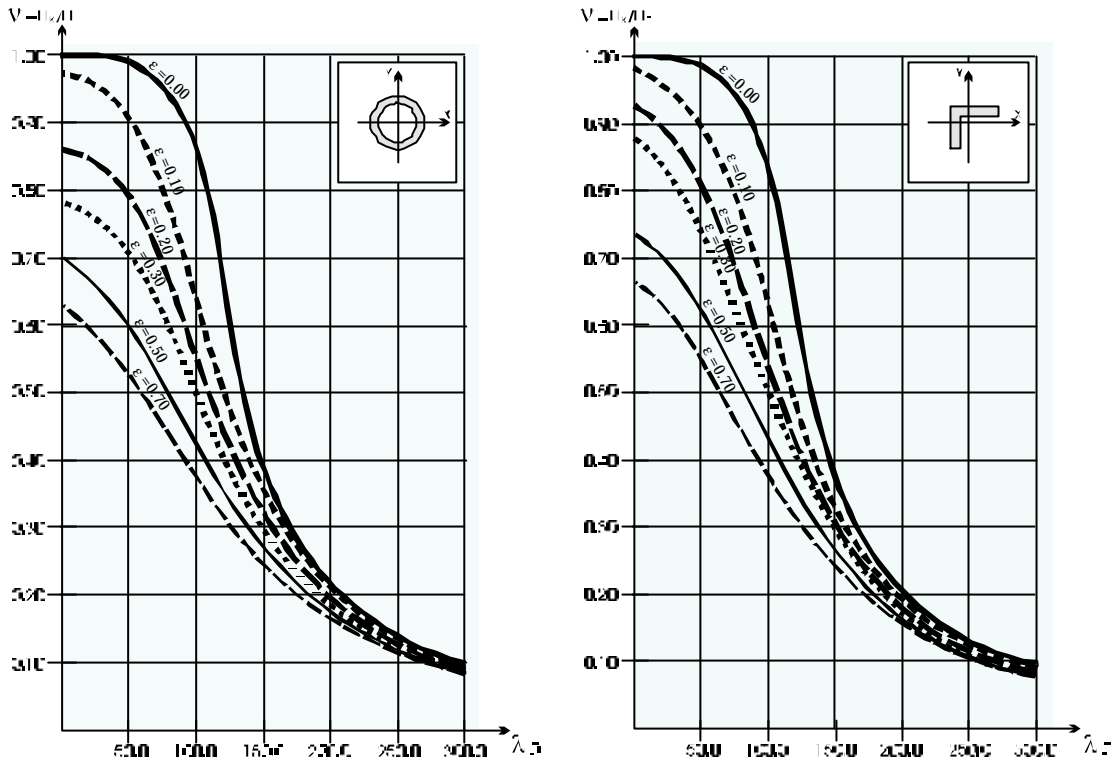


Fig. 9 Bearing capacity spectra for the hollow round and L-section [7]

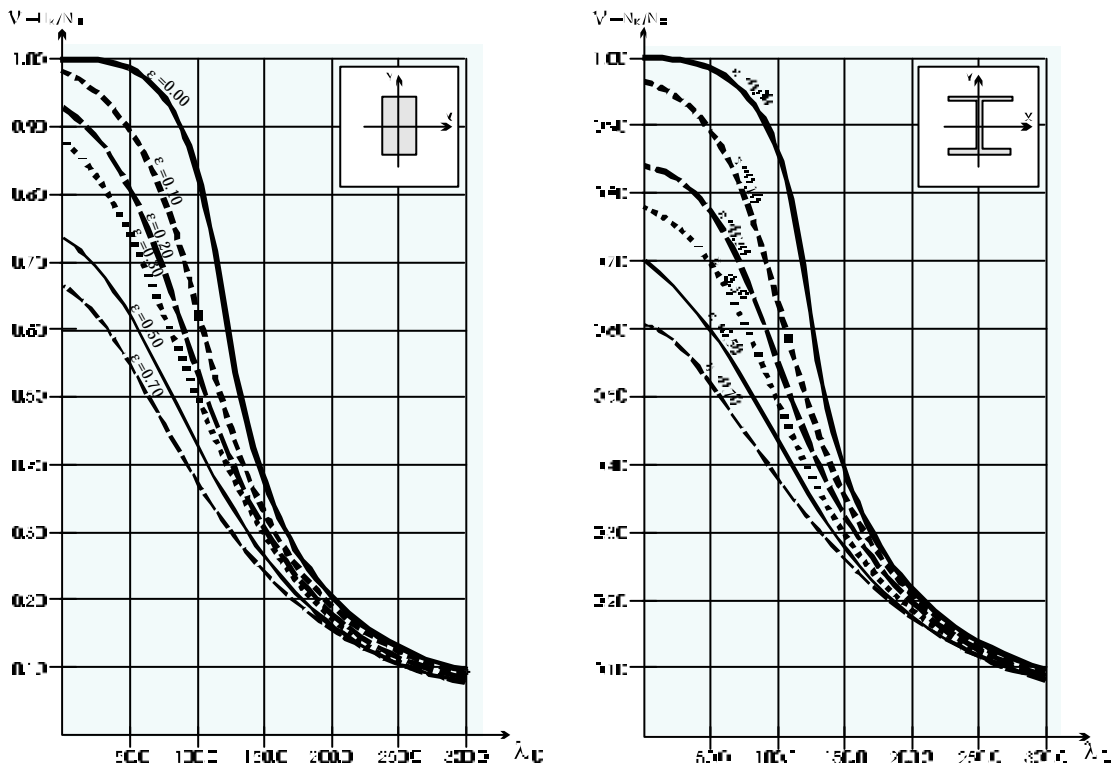


Fig. 10 Bearing capacity spectra for the full rectangular and I-section ( $h=b$ ) [7]

Now, for each group of sections a particular spectra diagram can be adopted as it can be seen in Figures 11, 12, 13 and 14.

After this procedure, all the obtained diagrams of bearing capacity spectra, based on the series of numerical experiments, can be used in the dimensioning procedure.

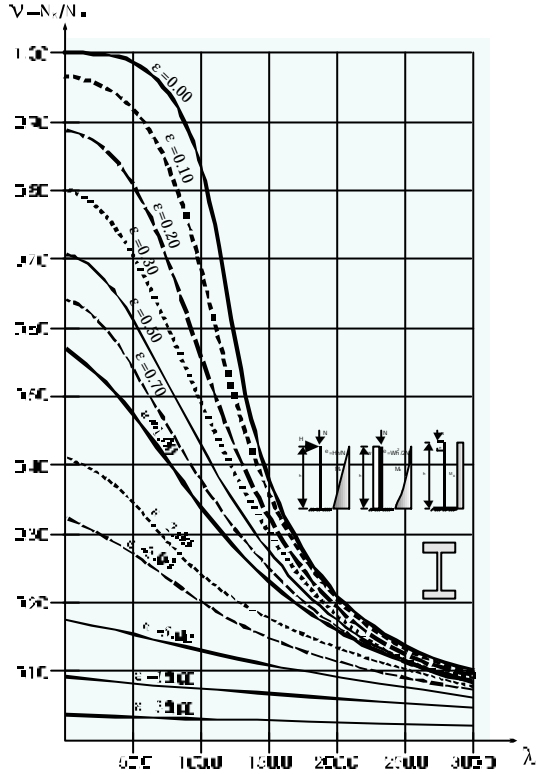


Fig. 11 Bearing capacity spectra of a steel column for I-sections  $h > b$  [7]

The results obtained by the nonlinear computation can be compared with those defined by DIN 18800 and EUROCODE 3. Figure 15 illustrates buckling curves according to the mentioned norms [8, 9].

The results of the nonlinear analysis are demonstrated in Figure 16.

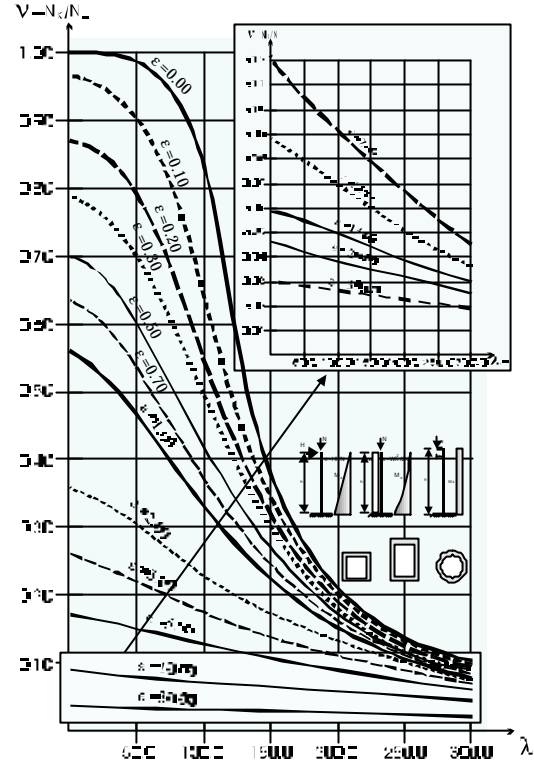


Fig. 12 Bearing capacity spectra of a steel column for all hollow sections [7]

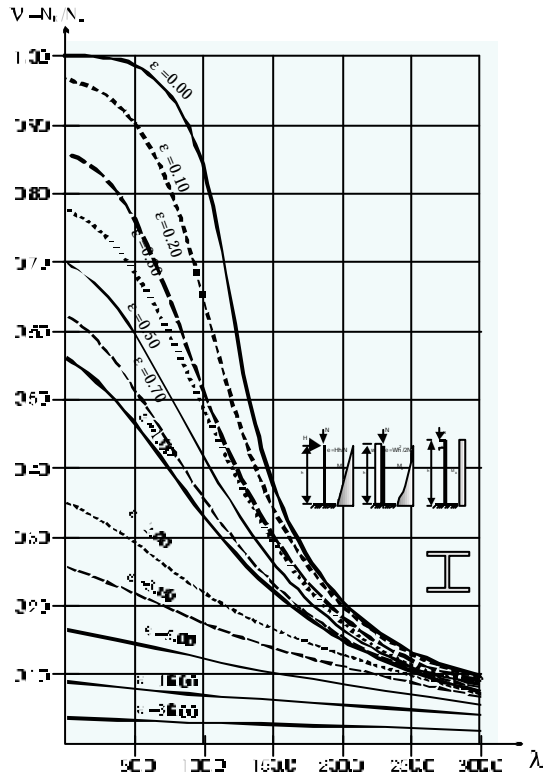


Fig. 13 Bearing capacity spectra of a steel column for »low« I-sections [7]

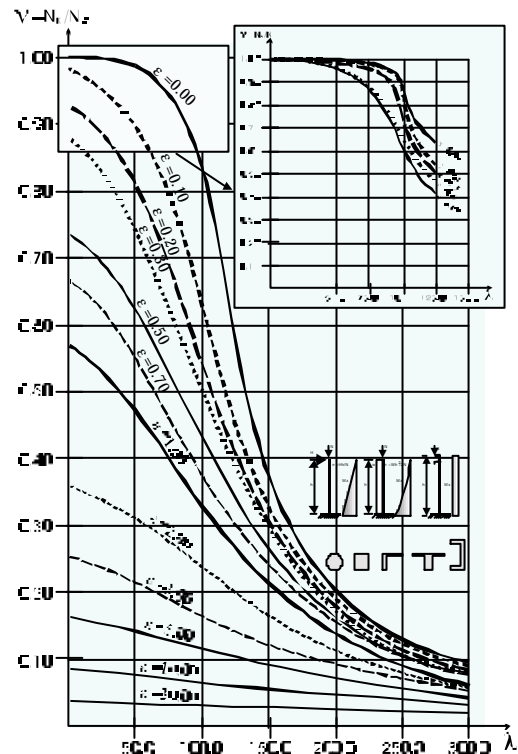


Fig. 14 Bearing capacity spectra of a steel column for: a) all full; b) unsymmetrical sections [7]

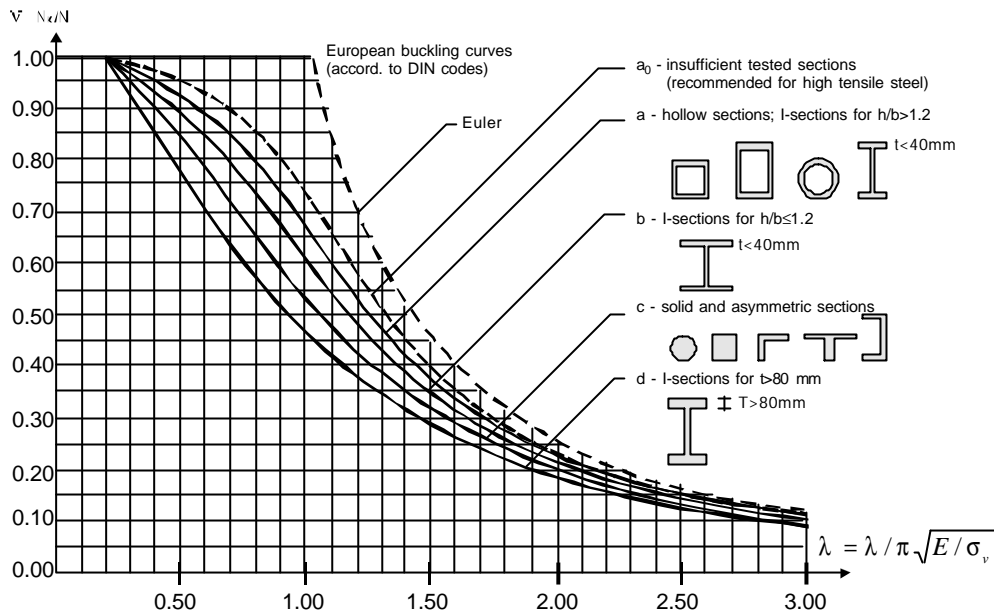


Fig. 15 Buckling curves according to EUROCODE 3, taken over from DIN 18800

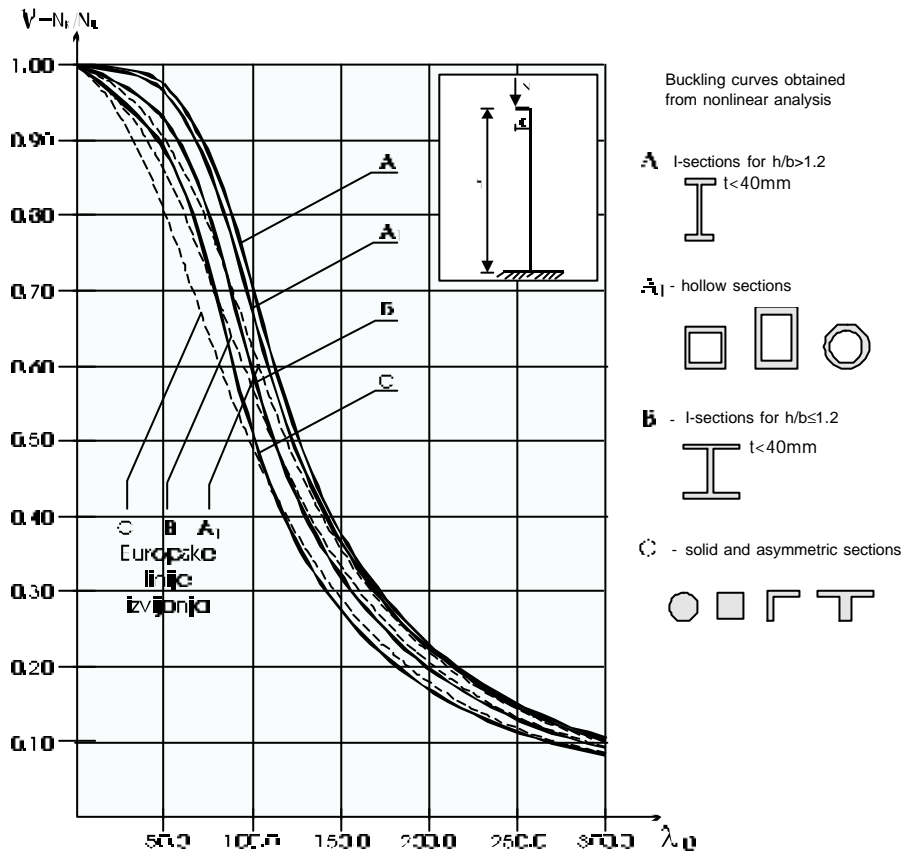


Fig. 16 Buckling curves obtained by nonlinear computation

#### 4. CONCLUSION

The analysis results are presented by non-dimensional diagrams which present the dependence of slenderness and critical force on the given eccentricity and they show that the sequence of buckling curves for individual sections is equivalent to the sequence defined by the above-mentioned rules.

Thus, it is proved that diagrams can be recommended for determining the bearing capacity of steel elements subject to eccentric load.

Diagrams obtained by geometrical and nonlinear models are applicable to all types of plain structures and available to engineers who need not have knowledge either of material or geometrical nonlinear models.



## 5. REFERENCES

- [1] A. Mihanoviæ and M. Schönauer, RAVNEL - computer program for the computation of plane frames, Faculty of Civil Engineering, University of Split, 1988.
- [2] J. Ožbolt and J. Dvornik, NELIN - Computer Program for Nonlinear Analysis of Combined Microcomputer, Proc. of the Int. Conf. on Computer Application in Concrete, Singapur, 1986.
- [3] M. Schönauer, Unified numerical analysis of cold and hot metal forming processes, Ph.D. Thesis, University of Wales, Department of Civil Engineering, Swansea, C/Ph/172/93, 1993.
- [4] M.A. Crisfield, *Finite Elements and Solution Procedures for Structural Analysis*, Pineridge Press, Swansea, 1986.
- [5] M.A. Crisfield, *Nonlinear Finite Element Analysis of Solids and Structure*, John Wiley and Sons, New York, 1991.
- [6] A. Mihanoviæ and M. Schönauer, Numerical model for stability analysis of frame structures with material and geometrical nonlinearity, *Int. J. for Eng. Mod.*, Vol. 4, No. 1-4, pp. 27-33, 1991.
- [7] A. Juriæ, Application of nonlinear numerical model for computing the bearing capacity and stability of steel structures, M.Sc. Thesis, Faculty of Civil Engineering, University of Split, 1998. (in Croatian)
- [8] B. Androiæ, B. Dujmoviæ and I. Džeba, *Steel Structures - 1*, Faculty of Civil Engineering, University of Zagreb, 1994. (in Croatian)
- [9] B. Androiæ, B. Dujmoviæ and I. Džeba, *Steel Structures - 2*, Faculty of Civil Engineering, University of Zagreb, 1995. (in Croatian)

## SPEKTRI DIJAGRAMA NOSIVOSTI ÈELIÈNIH KONSTRUKCIJA

### SAŽETAK

*U ovom radu prezentiran je postupak za dobivanje spektara dijagrama nosivosti kroz analizu stabilnosti elemenata štapnih èeliènih konstrukcija pomoæu materijalno i geometrijski nelinearnog modela. Spektri dijagrama su prikazani u bezdimenzionalnom obliku za svaku grupu popreènih presjeka, a predstavljaju ovisnost vitkosti i kritiène sile za zadani ekscentricitet. Rezultati analize usporeðeni su s postojećim normama iz područja stabilnosti èeliènih konstrukcija i pokazuju da su odstupanja minimalna. Dijagrami ne zahtijevaju posebne obuke ni znanja inženjera te su tako dostupni inženjerskoj praksi. U odnosu na klasiène proraèune, uporaba ovih dijagrama dobivenih uz uvažavanje materijalne i geometrijske nelinearnosti omogućuje racionalnije iskorištavanje materijala i konstrukcija.*

**Ključne rijeèi:** *materijalna i geometrijska nelinearnost, spektar dijagrama nosivosti, èeliène konstrukcije, analiza stabilnosti.*